Quantitative Biology 2021, 9(1): 73–83
https://doi.org/10.15302/J-QB-021-0233

RESEARCH ARTICLE

Testing the leanocentric locking-point theory by *in silico* partial lipectomy

Guanyu Wang*

[1] Department of Biology, School of Life Sciences, Southern University of Science and Technology, Shenzhen 518055, China
[2] Guangdong Provincial Key Laboratory of Computational Science and Material Design, Shenzhen 518055, China
* Correspondence: wanggy@sustech.edu.cn

Received December 6, 2020; Revised December 25, 2020; Accepted December 28, 2020

***Background*: The lipostatic set-point theory, ascribing fat mass homeostasis to leptin mediated central feedback regulation targeting the body's fat storage, has caused a variety of conundrums. We recently proposed a leanocentric locking-point theory and the corresponding mathematical model, which not only resolve these conundrums but also provide valuable insights into weight control and health assessment. This paper aims to further test the leanocentric theory.**

***Methods*: Partial lipectomy is a touchstone to test both the leanocentric and lipostatic theories. Here we perform *in silico* lipectomy by using a mathematical model embodying the leanocentric theory to simulate the long-term body fat change after removing some fat cells in the body.**

***Results*: The mathematical modeling uncovers a phenomenon called post-surgical fat loss, which was well-documented in real partial lipectomy surgeries; thus, the phenomenon can serve as an empirical support to the leanocentric theory. On the other hand, the leanocentric theory, but not the lipostatic theory, can well explain the post-surgical fat loss.**

***Conclusions*: The leanocentric locking-point theory is a promising theory and deserves further testing. Partial lipectomy surgeries are beneficial to obese patients for quite a long period.**

Keywords: leanocentric locking-point theory; lipostatic set-point theory; weight stability; fat mass homeostasis; partial lipectomy

Author summary: Our weight is generally very stable and this stability is believed to be a result of our brain regulating the body fat (lipostasis). We recently put forward a new theory (leanocentrism). To test both theories, we use mathematical modeling to simulate partial lipectomy surgeries and rediscover some phenomena (which are well-documented in real lipectomy surgeries) that can be well explained by leanocentrism but not lipostasis. Leanocentrism is thus promising and deserves further testing.

INTRODUCTION

Our body weight is remarkably stable. Even more than 100 years ago, Neumann noted stability of his own weight over more than a year, without conscious efforts to control his food intake or expenditure [1]. In his classic 1924 metabolism textbook, Eugene Dubois stated that "there is no stranger phenomenon than the maintenance of a constant body weight under marked variation in bodily activity and food consumption" [2]. Over the past several decades, rigorous perturbation experiments were performed to prove weight stability [3–12]. It was found that, although the weight value can be perturbed by persistent overfeeding or underfeeding, it always returns to the original value once the normal feeding is reinstated. Our weight is therefore truly stable. Because an ordinary adult's lean body mass is nearly invariant, weight stability is essentially about fat mass homeostasis. In this paper, we assume that the lean mass (LM) is strictly fixed; thus, the change in the body weight (BW) is strictly due to the

change in the fat mass (FM).

The lipostatic theory is a consensus theory to explain weight stability. In the theory, our body fat is under active regulation by the central nervous system (CNS) [13]. It has long been known that hunger and satiety are controlled by a small part of the brain called the hypothalamus [14]. But how does the hypothalamus know the body's adiposity level? The discovery of leptin in the 1990s fixed the missing link [15–17]. As a hormone secreted by adipocytes, leptin accurately and timely communicates the body's adiposity level to the brain, through activating its receptor primarily in the arcuate nucleus of the hypothalamus [18–21]. The leptin signal is compared with a hypothetical "set-point" in the hypothalamus, and the difference is used as the feedback signal to modulate energy intake (EI) and energy expenditure (EE) (Fig. 1A). This fat-leptin-hypothalamus axis has been widely accepted as the lipostat that keeps peoples' weight stable. The lipostatic setpoint theory is intuitively appealing and it is textbook knowledge today [22]. However, the lipostatic theory has many problems. The nature of the neuronal set-point, including its very existence, is totally unknown. The theory is also incompatible with a variety of empirical findings [10,23–28]. For example, it cannot explain well the phenomenon of middle-age spread (also known as set-point ratchet-up in the context of the lipostatic theory). To explain it, the concept of leptin resistance has to be invoked, but there are no solid evidence for leptin resistance. Taken together, despite its wide popularity, the lipostatic theory has not been proved [29].

In [28], we proposed a new theory, called *leanocentric locking-point theory*, which argues that leptin signaling and central regulation aim to ensure the lean tissues' energy requirement instead of the regulation of FM. In our body, the lean tissues provide the essential biological functions, which demand a high rate of energy supply and necessitate a central surveillance and coordination of all the energy depots in the body. Besides fat whose level is conveyed by leptin, the other energy substrates are also monitored, including plasma glucose (whose level is conveyed by insulin) and even food in the stomach (whose amount is conveyed by the hormone ghrelin). Insulin and ghrelin receptors were found on the same cells in the hypothalamus as the leptin receptors [30]. Integration of these signals allows the hypothalamus to perceive holistically the body's total energy status and to evaluate a suitable appetite so that the lean tissues' energy demand can be met timely. In summary, a new paradigm *leanocentrism* was formed, which maintains that the lean tissues' energy demand is what the CNS really cares (Fig. 1B).

We then developed a mathematical model (Eqs. (2)–(13)) to simulate the body's energy metabolism (Fig. 2), which also embodies the leanocentric principle [28]. We found that FM is largely determined by the lean tissues' properties, such as LM, TEE (total energy expenditure, which is primarily due to the lean tissues), and IR (the muscles' insulin resistance). The consistent change of any of these properties leads to the change of FM. This kind of determinstic weight change should not be construed as the destabilization of weight. Instead, weight stability is largely a cell-autonomous property of adipocytes, as we found from the modeling. In other words, fat mass homeostasis arises from each adipocyte's intrinsic self-tuning. That is, larger (smaller) adipocytes incline to shrink (expand). Although the adipocytes' mean size is "locked" by the lean tissues' properties, it can be

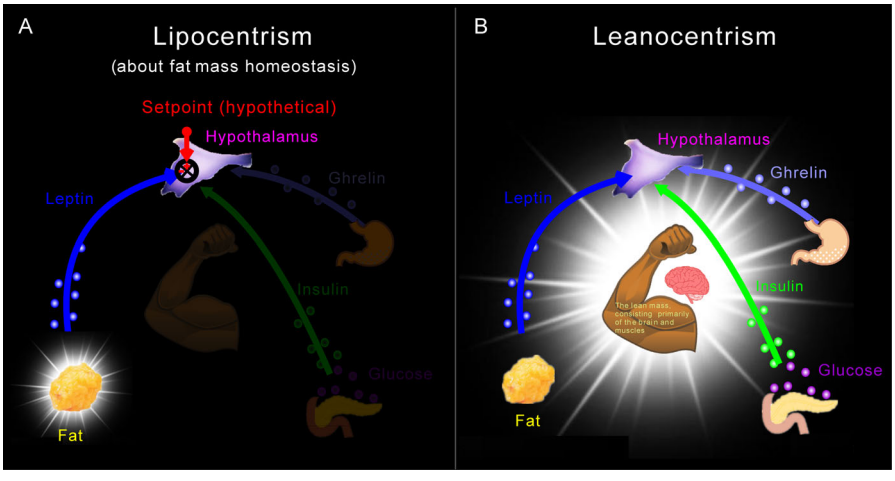

Figure 1. From lipocentrism to leanocentrism. (A) In the lipostatic theory, the body fat is the target of regulation, with the leptin concentration as the signal to be compared with a hypothetical set-point in the hypothalamus. (B) In the leanocentric paradigm, the lean body mass is the target of energy surveillance. Fat is only one of several energy substrates utilized by the lean tissues and monitored by the CNS.

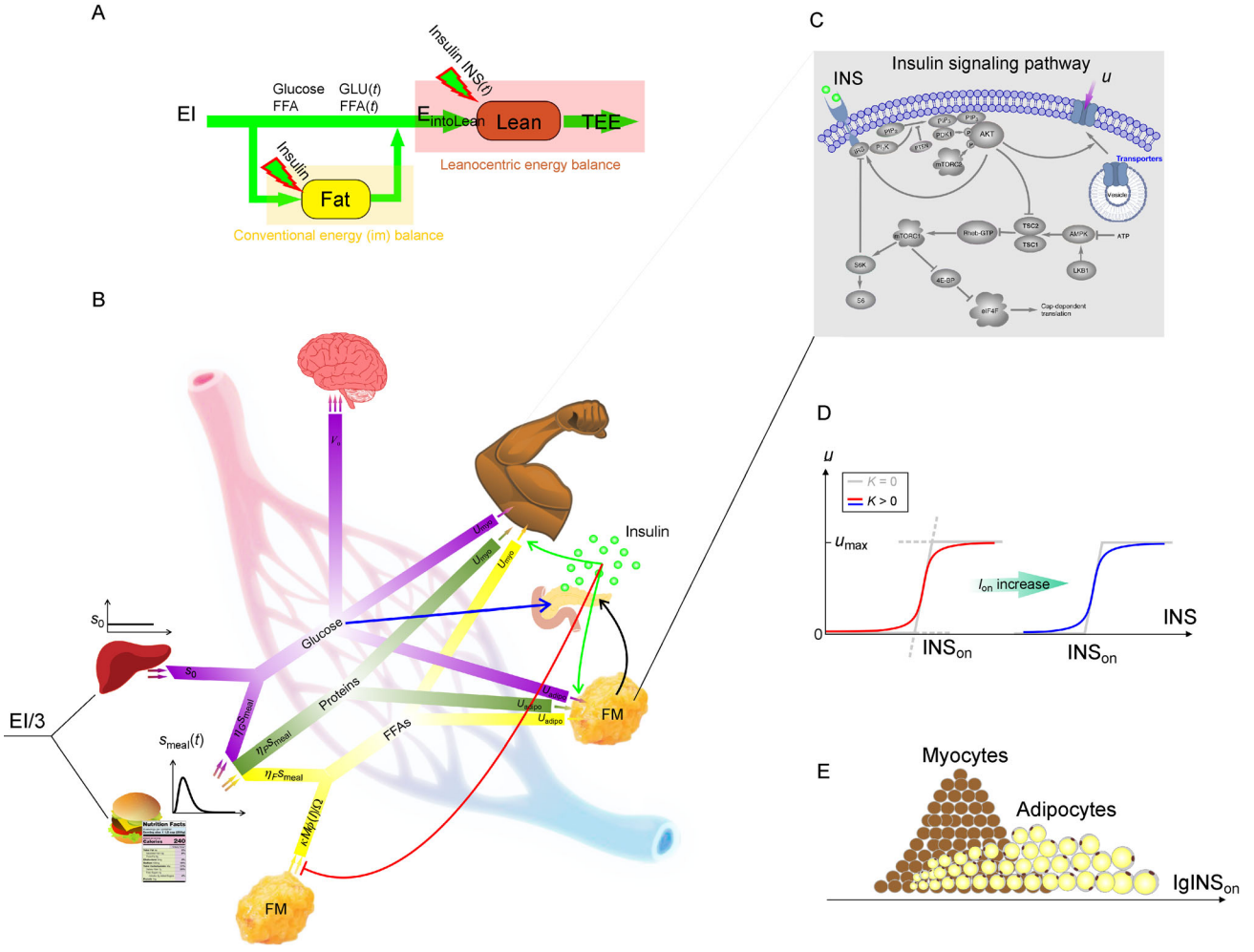

Figure 2. Peripheral dynamics. (A) Leanocentric energy balance as the overarching principle in peripheral dynamics. (B) Dynamical interplay among peripheral tissues, plasma insulin, and plasma nutrients. Plasma glucose (purple) is from either the liver or the meal, and is disposed primarily by the brain, muscles, and adipose tissues. The latter two's glucose disposal depends heavily on the plasma insulin (the green dots), which is secreted by the pancreas upon glucose stimulation (the blue arrow). The insulin secretion becomes greater as one becomes fatter (the black arrow). Amino acids (dark green) are from the meal. FFAs (yellow) are from either adipose tissues or the meal. They are disposed by muscles and adipose tissues, again depending on insulin. On the other hand, insulin inhibits lipolysis (the red bar-headed arrow). (C) Insulin signaling pathway. Upon binding to its receptor, insulin triggers a chain of molecular interactions inside the cell. The signal propagates through the cytoplasm and eventually renders the activation of Akt and the subsequent translocation of nutrient transporters to the plasma membrane, whereby nutrients can be massively transported into the cell. (D) The insulin response curve u(INS). Its shape is determined by the parameters of Eq. (9), namely K, α, $\mathrm{INS_{on}}$, and $u_{\max}$. As $\mathrm{INS_{on}}$ increases, the responses shift to the right. $K = 0$ corresponds to the limit condition as indicated, under which the response curve reduces to three straight lines. (E) The distribution of myocytes and adipocytes over the $\mathrm{lgINS_{on}}$ axis.

transiently increased (decreased) by *e.g.* intensive overfeeding (underfeeding). As long as the lean tissues' properties have not changed, the mean adipocyte size will gradually return to the locking point due to the adipocytes' self-tuning as soon as the overfeeding (underfeeding) is stopped.

In this paper, we further tested the leanocentric locking-point theory by performing *in silico* partial lipectomy. Partial lipectomy is a surgery removing some fat from the body for cosmetic or health benefits, which can be simulated by our mathematical model. The simulations gave rise to some interesting predictions. The predicted phenomena were actually observed in real lipectomy surgeries and can be well-explained by the leanocentric locking-point theory. Therefore, the results further validate the mathematical model and support the leanocentric locking-point theory. Importantly, the lipostatic set-point theory would predict entirely different phenomena, which, are against what were actually observed.

RESULTS AND DISCUSSIONS

Testing the lipostatic theory by *in silico* partial lipectomy

The lipostatic theory is mathematically simple because the whole system is a typical negative feedback system aiming to fix the fat mass. Therefore, the fat mass can be modeled by a single variable FM satisfying a rather generic equation:

$$\frac{\mathrm{dFM}}{\mathrm{d}t} = \lambda(\mathrm{FM}_0 - \mathrm{FM}), \tag{1}$$

where FM_0 is the "set-point" fat mass and $\lambda > 0$ is the feedback gain ensuring weight stability. Note that the term $-\lambda\,\mathrm{FM}$ reflects the fact that the negative feedback strength (the leptin concentration) is proportional to the fat mass, thus conforming with the lipostatic theory.

Let $\mathrm{FM}(0) = \mathrm{FM}_0$; namely, the fat mass is at the "set-point" at time 0. Now a $x\%$ lipectomy performed at time 0 results in a sudden drop of FM from FM_0 to $(1-x\%)\mathrm{FM}_0$ (indicated by the red arrow in Fig. 3A). According to Eq. (1), the fat mass will gradually return to FM_0 along the time course $\mathrm{FM}(t) = \mathrm{FM}_0(1 - x\% \cdot e^{-\lambda t})$ (Fig. 3, the red curve). That is, for the days after the surgery, the fat mass should increase consistently with an ever-decreasing rate of increase until finally return to FM_0. This result is easy to understand. According to the feedback control theory, the restoration force should be proportional to the deviation $\mathrm{FM}_0 - \mathrm{FM}$, which is the largest at time 0^+(*i.e.*, immediately after time 0). Therefore, weight rebound should be drastic in the beginning and gradually level off, just as illustrated by the red curve in Fig. 3A. This lipostasis-based prediction is however against the empirical observations (see below).

Testing the leanocentric locking-point theory by *in silico* partial lipectomy

In our mathematical model (Eqs. (2)–(13)), the fat tissue is represented by $N_{\mathrm{adipo}} = 2000$ *in silico* adipocytes. Therefore, a partial lipectomy can be simulated by randomly removing some *in silico* adipocytes from the system. For example, a 20% lipectomy corresponds to the random removal of 400 adipocytes from the 2000 total. We performed *in silico lipectomy* in three of the patients summarized in [28], namely, the patients 2, 3, and 13. For each patient, the lipectomy breaks the previous steady state and causes a round of dynamical change until a new steady state is established.

Patient 2 has IR = 1.8365 (see [28] for the quantification of insulin resistance), TEE = 2380 $\mathrm{kcal \cdot day^{-1}}$, and BW = 70.5 kg (FM = 17.5 and LM = 53.0). A 10% lipectomy was performed by randomly removing 200 adipocytes (which weighed 1.7 kg) from the 2000 total, with $N_{\mathrm{adipo}} = 1800$ adipocytes left in the body (which weighed 17.5 – 1.7 = 15.8 kg). The subsequent growth of the 1800 adipocytes was simulated. Quite surprisingly, FM continued to decrease for years until finally stabilized at around 15.2 kg, manifesting a significant, prolonged, post-surgical fat loss of 15.8 – 15.2 = 0.6 kg (Fig. 3D2, the red curve). This was unexpected because the lipostatic theory has predicted a virtually opposite change (the red curve in Fig. 3A). We then tested 20% lipectomy in patient 2 and again found the postsurgical fat loss of 14.0 – 13.0 = 1.0 kg (Fig. 3D2, the black curve).

Patient 3 has IR = 2.1830, TEE = 3100 $\mathrm{kcal \cdot day^{-1}}$, and BW = 132.1 kg (FM = 68.0 and LM = 64.1). A 5% lipectomy was performed by randomly removing 100 adipocytes (which weighed 3.4 kg) from the 2000 total, with $N_{\mathrm{adipo}} = 1900$ adipocytes left in the body (which weighed 68.0 – 3.4 = 64.6 kg). The subsequent growth of the 1900 adipocytes was simulated. We again found that FM continued to decrease until finally stabilized at around 57.3 kg, manifesting a significant postsurgical fat loss 64.6 – 57.3 = 7.3 kg (Fig. 3D3, the blue curve). Note that the 7.3 kg post-surgical fat loss was much larger than the excised fat (3.4 kg), a phenomenon not observed from patient 2. We then tested 10% lipectomy in patient 3, which led to 61.2 – 48.7 = 12.5 kg of postsurgical fat loss (Fig. 3D3, the red curve). Again, the 12.5 kg post-surgical fat loss was much larger than the excised 6.8 kg fat (68.0 – 61.2 = 6.8).

Patient 13 has IR = 2.1132, TEE = 2528 $\mathrm{kcal \cdot day^{-1}}$, and BW = 82.9 kg (FM = 37.7 and LM = 45.2). A 5% lipectomy was performed by randomly removing 100 adipocytes (which weighed 1.9 kg) from the 2000 total, with $N_{\mathrm{adipo}} = 1900$ adipocytes (which weighed 37.7 – 1.9 = 35.8 kg) left in the body. We again found that FM continued to decrease until finally stabilized at around 33.8 kg, manifesting a significant post-surgical fat loss 35.8 – 33.8 = 2.0 kg (Fig. 3D13, the blue curve). Note that the 2.0 kg post-surgical fat loss was comparable to the excised fat (1.9 kg). We then tested 10% lipectomy in patient 13, which led to 33.9 – 30.4 = 3.5 kg of post-surgical fat loss (Fig. 3D13, the red curve). Again, the 3.5 kg post-surgical fat loss was comparable to the excised 3.8 kg fat (37.7 – 33.9 = 3.8).

The above lipectomy-induced dynamics have some salient features.

• *Post-surgical fat loss*. After the surgery, FM continued to decrease for a long period until finally stabilized at a minimal value. Moreover, the fatter the patient, the more drastic the post-surgical fat loss. This phenomenon is rather counterintuitive. One would expect that the fat mass will gradually increase and finally return to the pre-surgical level, as predicted by the lipostatic theory.

• *Absence of fat restoration*. FM finally stabilized at the minimal value. It never increased, let alone returning to the pre-surgical level.

• *Negligible change of food intake*. During the running of the model, the *condition necessary feeding* (*i.e.*, EI is just sufficient for TEE) was applied. Note that necessary feeding does not necessarily mean EI = TEE. See [28] for the detailed explanation. By this condition, the magnitude A of the meal supply function was calculated over the course of time. It turned out that the *in silico* lipectomy did not lead to significant changes of the amount of meal (Fig. 3E2, 3E3, 3E13). Therefore, the post-surgical fat loss was not caused by the reduced food amount of the patients after the surgery.

The predicted phenomena are supported by empirical findings

To verify the computational predictions, we performed a survey in the literature about partial lipectomy [31–37]. We found, amazingly, that these real surgeries support what we predicted.

• *Post-surgical fat loss*. Crahay and Nizet interrogated five databases and found 40 articles (12 experimental animal studies and 28 human studies) on suction-assisted lipectomy satisfying certain selection criteria [37]. All the 40 articles pointed out that, after suction-assisted lipectomy, the body weight continued to decrease, and the weight loss was due to the reduced FM only (*i.e.*, LM does not change). Therefore, post-surgical fat loss is apparently a ubiquitous phenomenon. Moreover, in a study involving mesenteric visceral lipectomy in four non-diabetic obese baboons, although only an average of 0.43 kg of adipose tissue was removed, FM decreased by an average of 1.9 kg at six-week follow-up [38]. That is, post-surgical fat loss was about 1.47 kg, much more than the 0.43 kg excised part. This corresponds well to the *in silico* lipectomy in patients 3 and 13, which also led to the postsurgical fat loss more than the excised part. Another example was about testing the effect of 24% lipectomy to nonobese adult Sprague-Dawley rats [32]. Two groups of rats were tested: the lipectomized (sham-operated) group with presurgical weights of 357 ± 4 (363 ± 3) gram. For the lipectomized group, 13 gram of adipose tissue was removed, resulting in an additional loss of 20 gram and the minimal weight being $357-13-20=324$ gram. For the sham-operated group, there was a negligible change of weight from 363 ± 3 gram to 361 ± 3 gram. This experiment again demonstrated the phenomenon of postsurgical fat loss. Moreover, the fat loss was not due to the surgical trauma, because the sham-operated rats had only slight (2 gram) weight loss. Taken together, the empirical data consistently demonstrate that fat loss continues after partial lipectomy; they strongly support our mathematical model.

• *Absence of fat restoration*. Similar to our model predictions, fat restoration was indeed absent in some experiments (Fig. 3A, the solid black curve) [36,39,40]. However, the scenario was different in some other experiments [33,41,42], in which fat restoration was actually observed in the end (Fig. 3A, the dashed black curve).

• *Negligible change of food intake*. This finding corresponds well to the practice. There are no reports about altered food intake induced by lipectomy, to the best of our knowledge. In fact, several experiments paid close attention to this issue but failed to detect a change of food intake caused by partial lipectomy [42,43].

Physiologic mechanisms underlying the observed phenomena

Post-surgical fat loss

The post-surgical fat loss, although consistently reported, was not explained. Nobody even noticed its incompatibility with the lipostatic theory, according to which the weight should rebound immediately to compensate for the excised fat (Fig. 3A, the red curve). The restoring force should be the strongest in the beginning, because according to the feedback control theory, the force should be proportional to the deviation from the set-point, which is the largest at the moment immediately after the surgery. Against such a strong force of weight rebound, the post-surgical fat loss has no chance to occur. Therefore, the post-surgical fat loss phenomenon is directly against the lipostatic theory.

The post-surgical fat loss can be well explained by leanocentrism, according to which satisfaction of the lean tissues' energy demand is always the urgent task of our CNS. In our body, the energy is supplied by the nutrients in the blood, including plasma glucose, amino acids, and free fatty acids (FFAs). Because FFAs are secreted by the body fat store, the sudden reduction of the body fat store by partial lipectomy is a critical event: it immediately causes a state of energy deficit of the lean tissues. If the body kept a normal rate of lipolysis, then this energy deficit state would persist (Fig. 3B). To eliminate the deficit, the remaining fat store has to accelerate lipolysis and consequentially becomes significantly smaller (Fig. 3C). In other words, the post-surgical fat loss is due to accelerated lipolysis of the remaining fat to compensate for the energy expenditure originally supplied by the excised fat. Everything centers on the lean tissues.

The physiologic underpinning of the accelerated lipolysis can be well explained. Lipolysis is inhibited by the plasma insulin (Fig. 2B, the red bar-headed arrow);

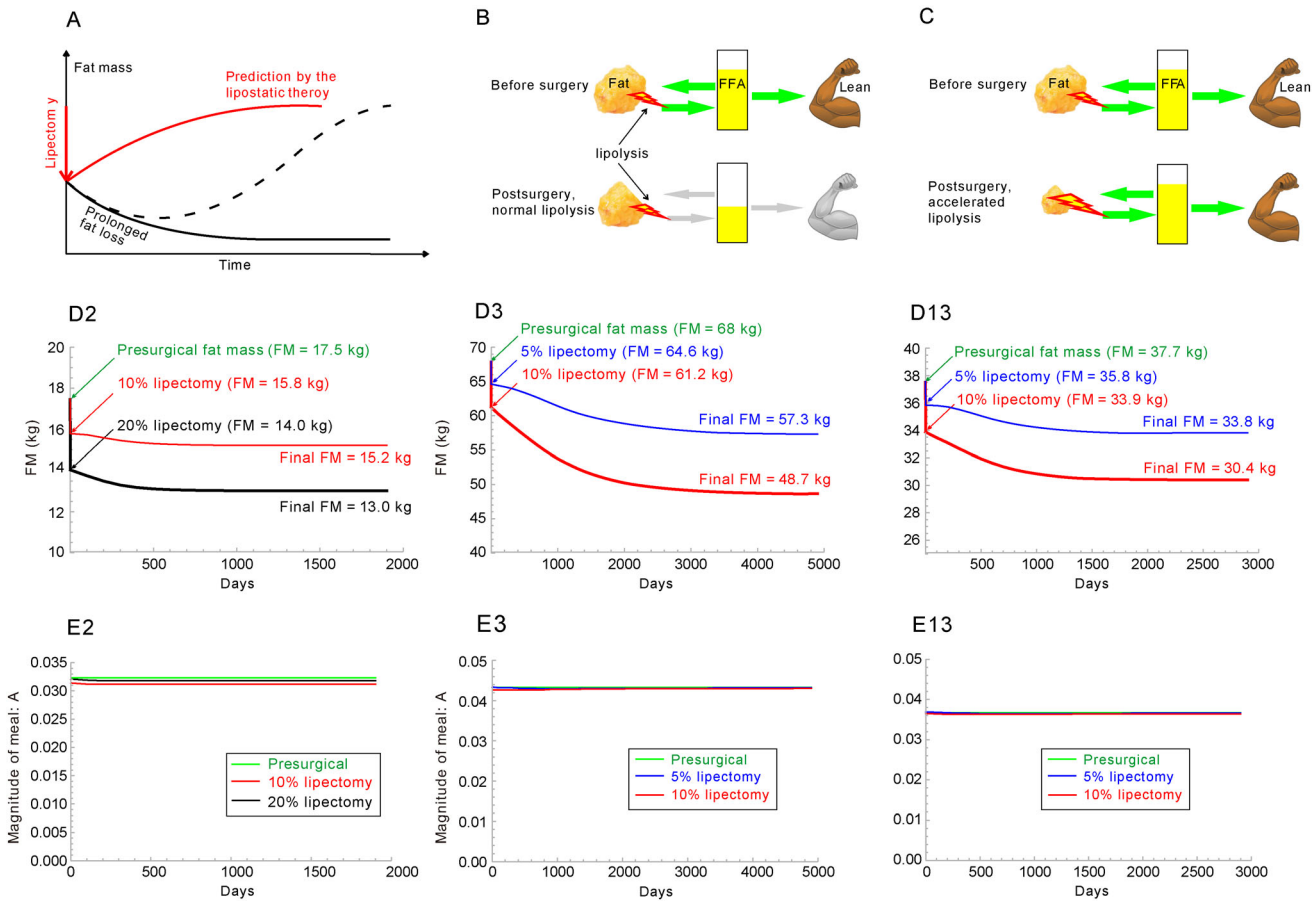

Figure 3. Consequences of partial lipectomy. Subfigures labeled with 2, 3, or 13 present computer simulations on subjects 2, 3, or 13, respectively. (A) According to clinical practice and animal experiments, the body continues to lose fat after the surgery for quite some time (black curves), which may (the dashed curve) or may not (the solid black curve) be followed by fat restoration. The observations are at odds with the prediction by the lipostatic theory (the red curve). (D2, D3, D13) Fat mass dynamics after partial lipectomy, which have demonstrated the post-surgical fat loss. (E2, E3, E13) The magnitude of food intake. There is a negligible change of food intake after the lipectomy. The following explains the post-surgical fat loss. (B) Before the surgery, the rates of FFA transmission are all normal. After the surgery, because the fat mass becomes smaller, all the rates of FFA transmission become smaller, as well as the plasma FFAs concentration. As a consequence, the lean tissues would be in a state of energy deficit. (C) To avoid the energy deficit, the adipose tissues accelerate lipolysis, which raises all the rates of FFA transmission to the normal level. The expense is the post-surgical fat loss.

thus a reduction of plasma insulin concentration can accelerate lipolysis. It turns out that lipectomy can reduce plasma insulin concentration by reducing the secretion of insulin. Indeed, the insulin secretion modulator ψ (FM) (see Eq.(S15) of [28]) is a monotonic increasing function of the fat mass. After the lipectomy, FM is reduced, as well as ψ (FM). This reduced secretion of insulin makes the plasma insulin concentration decrease. Lipolysis consequentially accelerates, which causes the post-surgical fat loss.

The phenomenon of post-surgical fat loss demonstrates a clinical benefit of partial lipectomy: the weight keeps reducing for quite a long period as long as the patient keeps necessary feeding. Because the physiologic mechanisms of the post-surgical fat loss have been revealed in the last paragraph, it is possible to maximize the fat loss and to achieve the maximal clinical benefits based on the revealed physiologic mechanisms.

Negligible change of food intake

The negligible change of food intake and the post-surgical fat loss are the two sides of the same coin. Now that the body can maximize endogenous energy utilization by accelerating lipolysis, it does not rely on the increase of exogenous energy. Acceleration of lipolysis is a more immediate action and thus often preempts meal ingestion. That is, before the meal time, the acceleration of lipolysis has already compensated the energy deficit, which makes it unnecessary to increase food intake. This is again at

odds with the lipostatic theory, which predicts significant increase of food intake for the restoration of fat.

Absence or presence of fat restoration

Both absence and presence of fat restoration were observed following real lipectomy surgeries. For fat restoration to occur, it is required that new adipocytes can be generated from local precursor cells [40]. Therefore, fat restoration depends heavily on the conditions after the surgery. If the condition for adipocyte regeneration is ideal, then a full restoration will be finally achieved, after some post-surgical fat loss (Fig. 3A, the dashed curve). If the condition is moderately good, then partial fat restoration might be observed. If the nutritional conditions are poor, then the recruitment of pre-adipocytes is inhibited, and thus the fat is not restored during the period of observation (Fig. 3A, the solid black curve).

In our modeling results (Fig. 3D), the number of adipocytes N_{adipo} was fixed at $(1–x\%)\cdot$ 2000, namely, no adipocyte regeneration, which explains the absence of fat restoration. If N_{adipo} is changed to 2000, then full fat restoration will be observed. Therefore, the leanocentric model can explain both observations: non-compensation [36,39,40] corresponds to the fixed N_{adipo} $=(1–x\%)\cdot$ 2000 and compensation [33,41,42] corresponds to the gradual increase of N_{adipo} from $(1–x\%)\cdot$ 2000 to 2000 during the model run.

Finally, note that fat restoration should not be construed as fat mass homeostasis. It is essentially cell number homeostasis (*i.e.*, the number of adipocytes of an adult is generally very constant [44]).

CONCLUSION

Fat mass homeostasis is traditionally considered from a lipostatic perspective, which emphasizes the feedback signal (leptin) from the body fat to the hypothalamus (the lipostatic set-point theory). We recently proposed a leanocentric locking-point theory, which seems more promising than the lipostatic theory [28]. Mathematical modeling proves to be an effective tool to uncover mechanisms from the immense complexities of biological systems [45]. We therefore tested both theories by using the corresponding mathematical models to simulate the long-term body fat change after a partial lipectomy surgery. The results show qualitatively different dynamical patterns: the immediate fat rebound in the lipostatic theory (Fig. 3A, the red curve) and the continued fat loss in the leanocentric theory (Fig. 3B, the black solid curve). It is well-known that qualitative difference is important to distinguish different mechanisms [46,47]; thus, the *in silico* lipectomy did reveal important phenotype differences between the two theories. For the leanocentric theory, we have found interesting phenomena such as post-surgical fat loss, absence of fat restoration, and negligible change of food intake. These phenomena were well-documented in real partial lipectomy surgeries, thus serving as empirical supports to the leanocentric theory. Moreover, the leanocentric theory and the details of the mathematical model can well-explain these phenomena. For the lipostatic theory, we found it difficult to explain these phenomena, especially the post-surgical fat loss. Therefore, the leanocentric locking-point theory is much more promising than the lipostatic theory and thus deserves further testing.

MATERIALS AND METHODS

Mathematical model

Part 1. Dynamics of plasma glucose, FFAs, amino acids, and insulin

$$\frac{\mathrm{dGLU}}{\mathrm{d}t}=\eta_{\mathrm{GLU}}\cdot S_{\mathrm{meal}}+s_0 -(V_{\mathrm{GLU0}}+U_{\mathrm{myo}}+U_{\mathrm{adipo}})\mathrm{GLU}, \tag{2}$$

$$\frac{\mathrm{dFFA}}{\mathrm{d}t}=\eta_{\mathrm{FFA}}\cdot S_{\mathrm{meal}}+\kappa\cdot\mathrm{FM}\cdot\phi(I)/\Omega -(V_{\mathrm{FFA0}}+U_{\mathrm{myo}}+U_{\mathrm{adipo}})\mathrm{FFA}, \tag{3}$$

$$\frac{\mathrm{dAA}}{\mathrm{d}t}=\eta_{\mathrm{AA}}\cdot S_{\mathrm{meal}}-(V_{\mathrm{AA0}}+U_{\mathrm{myo}}+U_{\mathrm{adipo}})\mathrm{AA}, \tag{4}$$

$$\frac{\mathrm{dINS}}{\mathrm{d}t}=\psi(\mathrm{FM})\cdot(r+f(\mathrm{GLU}))-\kappa\mathrm{INS}, \tag{5}$$

$$U_{\mathrm{myo}}=\sum_{j=1}^{N_{\mathrm{myo}}}u_j, \tag{6}$$

$$U_{\mathrm{adipo}}=\sum_{i=1}^{N_{\mathrm{adipo}}}u_i, \tag{7}$$

$$\mathrm{FM}=\sum_{i=1}^{N_{\mathrm{adipo}}}m_i, \tag{8}$$

where

GLU is the plasma glucose concentration.

FFA is the plasma free fatty acids concentration.

AA is the plasma amino acids concentration.

INS is the plasma insulin concentration.

S_{meal} is the source rate of nutrients supplied by the

meal; it is further described by Eq. (S13) of [28].

s_0 is the source rate of glucose supplied by the liver.

η_{GLU}, η_{FFA}, and η_{AA} are the mass percentages of glucose, fat, and protein, respectively, in the meal.

V_{GLU0} is the basal (non-insulin dependent) rate of glucose intake by the whole body. It is contributed primarily by the brain, which can utilize glucose actively in the absence of insulin.

V_{FFA0} is the basal (non-insulin dependent) rate of FFA intake.

V_{AA0} is the basal (non-insulin dependent) rate of intake of amino acids.

U_{myo} is the muscles' rate of nutrient intake in response to insulin stimulation. It sums up from individual myocytes (Eq. (6)).

u_j is the rate of insulin mediated nutrient intake by the j-th myocyte. The function $u_j(\mathrm{INS})$ is constrained by Eq. (9).

N_{myo} is the number of *in silico* myocytes.

U_{adipo} is the adipose tissues' rate of nutrient intake in response to insulin stimulation. It sums up from individual adipocytes (Eq. (7)).

u_i is the rate of insulin mediated nutrient intake by the i-th adipocyte. The function $u_i(\mathrm{INS})$ is constrained by Eq. (9).

N_{adipo} is the number of *in silico* adipocytes.

FM represents the fat mass. It sums up from individual adipocytes (Eq. (8)).

m_i is the mass of the i-th adipocyte.

κ is the rate of lipolysis.

ϕ (INS) is a function of insulin inhibiting lipolysis; it is further described by Eq. (S16) of [28].

Ω is the body's volume of blood.

r is the basal rate of pancreatic insulin secretion.

f (GLU) is the rate of pancreatic insulin secretion in response to glucose stimulation; it is further described by Eq. (S14) of [28].

ψ (FM) is a function of fat mass promoting insulin secretion. It takes into account the fact that both basal and glucose-stimulated insulin secretion increase as one becomes fatter. It is further described by Eq. (S15) of [28].

k is the rate of insulin degradation.

Part 2. Insulin response curve u(INS) of an adipocyte or myocyte

$$0=\frac{\alpha}{\mathrm{INS}_{\mathrm{on}}}\left(\frac{u}{u_{\max}}\right)^3+\left((K-1)\frac{\alpha}{\mathrm{INS}_{\mathrm{on}}}+\frac{\mathrm{INS}}{\mathrm{INS}_{\mathrm{on}}}-1\right)\left(\frac{u}{u_{\max}}\right)^2+\left(K+1+(K-1)\frac{\mathrm{INS}}{\mathrm{INS}_{\mathrm{on}}}-K\frac{\alpha}{\mathrm{INS}_{\mathrm{on}}}\right)\frac{u}{u_{\max}}-K\frac{\mathrm{INS}}{\mathrm{INS}_{\mathrm{on}}},\tag{9}$$

$$u_{\max}=(V_{\max}-V_{\mathrm{GLU0}})/(N_{\mathrm{adipo}}+N_{\mathrm{myo}}).$$

This equation, obtained by mathematical modeling of insulin signaling pathway [48–50], gives rise to the sigmoidal curves in Fig. 2D. Here

INS is the plasma insulin concentration (the stimulus).

u is the cell's rate of insulin mediated nutrient intake (the response).

α, $\mathrm{INS}_{\mathrm{on}}$, K are the three parameters determining the shape of u(INS); in particular, $\mathrm{INS}_{\mathrm{on}}$ has the meaning of insulin response threshold and is defined as the cell's degree of insulin resistance.

$u_{\max}$ is the cell's maximal rate of insulin mediated nutrient intake.

$V_{\max}$ is the maximal rate of glucose intake by the whole body. It can be estimated from the whole body's data [51].

V_{GLU0} is the basal (non-insulin dependent) rate of glucose intake by the whole body.

The above symbols are often followed by a subscript: i to indicate adipocyte and j to indicate myocyte. For example, u_i is the nutrient intake rate of the i-th adipocyte; $(\mathrm{INS}_{\mathrm{on}})_j$ is the $\mathrm{INS}_{\mathrm{on}}$ of the j-th myocyte.

Part 3. Dynamics of adipocyte growth

$$\frac{\mathrm{d}m_i}{\mathrm{d}t}=(u_i\cdot(\mathrm{GLU}+\mathrm{FFA}+\mathrm{AA})+u_{\mathrm{FFA0}}\mathrm{FFA}+u_{\mathrm{AA0}}\mathrm{AA})\cdot\Omega-\kappa\cdot m_i\cdot\phi(\mathrm{INS}),\tag{10}$$

$$m_i=\zeta\cdot(\mathrm{INS}_{\mathrm{on}})_i,\tag{11}$$

where

$u_{\mathrm{FFA0}}=V_{\mathrm{FFA0}}/(N_{\mathrm{myo}}+N_{\mathrm{adipo}})$ is a cell's basal intake rate of FFAs.

$u_{\mathrm{AA0}}=V_{\mathrm{AA0}}/(N_{\mathrm{myo}}+N_{\mathrm{adipo}})$ is a cell's basal intake rate of amino acids.

m_i is the mass of the i-th adipocyte.

$(\mathrm{INS}_{\mathrm{on}})_i$ is $\mathrm{INS}_{\mathrm{on}}$ of the i-th adipocyte.

ζ is the scale factor between $\mathrm{INS}_{\mathrm{on}}$ and m.

Part 4. Leanocentric energy balance

$$\frac{E_{\mathrm{intoLean}}}{3}=\frac{\mathrm{TEE}}{3},\tag{12}$$

where

$$\frac{E_{\mathrm{intoLean}}}{3}=\int_0^T(\rho_{\mathrm{GLU}}V_{\mathrm{GLU0}}\mathrm{GLU}\Omega+\rho_{\mathrm{GLU}}U_{\mathrm{myo}}\mathrm{GLU}\Omega+\rho_{\mathrm{FFA}}\cdot u_{\mathrm{FFA0}}\cdot N_{\mathrm{myo}}\mathrm{FFA}\Omega+\rho_{\mathrm{FF}A}U_{\mathrm{myo}}\mathrm{FFA}\Omega+\rho_{\mathrm{AA}}\cdot u_{\mathrm{AA0}}\cdot N_{\mathrm{myo}}\mathrm{AA}\Omega+\rho_{\mathrm{AA}}U_{\mathrm{myo}}\mathrm{AA}\Omega)\mathrm{d}t,\tag{13}$$

where

E_{intoLean} is the energy entering the lean tissues in a day.

TEE represents the total energy expenditure in a day.

T is the meal cycle, namely the period starting with a meal and ending just before the next meal. Assuming a day is equally divided by the three meals, one has $T = 8$ h $= 480$ min.

ρ_{GLU}, ρ_{FFA}, and ρ_{AA} are the energy densities of glucose, fat, and protein, respectively.

Model parameters

The parameter values are presented in Table 1.

Table 1 Canonical parameter values

Parameter	Value	Unit	Remark
T	480.0	min	The meal cycle. By apportioning one day to the three meal cycles, one obtains T = 8 h = 480 min
FFA_0	1.25×10^{-4}	$\text{kg}\cdot\text{L}^{-1}$	The fasting FFA level. Taken from [52]
GLU_0	9.50×10^{-4}	$\text{kg}\cdot\text{L}^{-1}$	The fasting glucose level. Taken from [53]
INS_0	8.00	$\mu\text{U}\cdot\text{mL}^{-1}$	The fasting insulin level. Taken from [53]
σ_{myo}	0.35	$\lg(\mu\text{U}\cdot\text{mL}^{-1})$	The standard deviation of the normal distribution of the myocytes' $\lg(\text{INS}_{\text{on}})$ values. It usually pairs with IR to represent the normal distribution, namely (IR, σ_{myo}). The value 0.35 was taken from [54]
V_{GLU0}	0.0207	min^{-1}	Estimated from Fig. 1 of [51]
$V_{\max}$	0.139	min^{-1}	Estimated from Fig. 1 of [51]
$u_{\max}$	1.183×10^{-5}	min^{-1}	It equals $(V_{\max} - V_{\text{GLU0}})/(N_{\text{adipo}} + N_{\text{myo}})$
$\mu_{u_{\max}}$	1.183×10^{-5}	min^{-1}	The mean of $u_{\max}$ when it is randomized
$\sigma_{u_{\max}}$	6.00×10^{-6}	min^{-1}	The standard deviation of $u_{\max}$ when it is randomized
V_{FFA0}	0.200	min^{-1}	Taken from [52]
u_{FFA0}	2×10^{-5}	min^{-1}	It is estimated from $V_{\text{FFA0}} = (N_{\text{adipo}} + N_{\text{myo}})$
V_{AA0}	0.118	min^{-1}	Taken from [55]
u_{AA0}	1.18×10^{-5}	min^{-1}	It is estimated from $V_{\text{AA0}} = (N_{\text{adipo}} + N_{\text{myo}})$
κ	1×10^{-5}	min^{-1}	Estimated in [28]
Ω	5.0	L	An adult's blood volume is about 5 liters [56]
$\rho_{GLU}, \rho_{FFA}, \rho_{AA}$	4200, 9400, 4700	$\text{kcal}\cdot\text{kg}^{-1}$	Energy densities of glucose, fat, and protein [57]
$\eta'_{\text{GLU}} : \eta'_{\text{FFA}} : \eta'_{\text{AA}}$	0.500 : 0.300 : 0.200	dimensionless	Calorie percentage of glucose, fat, and protein in the food
$\eta_{\text{GLU}} : \eta_{\text{FFA}} : \eta_{\text{AA}}$	0.615 : 0.165 : 0.220	dimensionless	Mass percentage of glucose, fat, and protein in the food, which can be converted from calorie percentage by $\eta_i = \eta'_i / \rho_i / (\eta'_{\text{GLU}}/\rho_{\text{GLU}} + \eta'_{\text{FFA}}/\rho_{\text{FFA}} + \eta'_{\text{AA}}/\rho_{\text{AA}})$, for i = GLU, FFA, AA
s_0	2×10^{-5}	$\text{kg}\cdot\text{L}^{-1}\cdot\text{min}^{-1}$	Steady state condition $s_0 = V_{\text{GLU0}} G_0 = 2 \times 10^{-5}$
k	0.322	min^{-1}	Taken from [54], with adjustment
$f_{\max}$	35.52	$\mu\text{U}\cdot\text{mL}^{-1}\text{min}^{-1}$	Taken from [54], with adjustment
GLU_h	1.443×10^{-3}	$\text{kg}\cdot\text{dL}^{-1}$	Taken from [54], with adjustment
n	6.432	dimensionless	Taken from [49,54], with adjustment
r	0.285	$\mu\text{U}\cdot\text{mL}^{-1}\text{min}^{-1}$	Steady state condition $r = k \cdot INS_0 - f(GLU_0) = 0.285$
τ_1	19.03	min	Taken from [49,54], with adjustment
τ_2	40.20	min	Taken from [49,54], with adjustment
τ_3	103.2	min	Taken from [49,54], with adjustment
b	4.064	dimensionless	Taken from [49,54], with adjustment
c	0.0482	min^{-1}	Taken from [49,54], with adjustment
ψ_0	0.4265	dimensionless	Estimated in [28]
ψ_1	3.443×10^{-2}	kg^{-1}	Estimated in [28]
N_{myo}	8000	dimensionless	The number of *in silico* myocytes
N_{adipo}	2000	dimensionless	The number of *in silico* myocytes
α	−4.000	dimensionless	Standard value used in [48]
K	0.050	dimensionless	Standard value used in [48]
INS_h	7.3	$\mu\text{U}\cdot\text{mL}^{-1}$	IC50 of insulin inhibiting lipolysis. Taken from [58]

(*Continued*)

Parameter	Value	Unit	Remark
n_0	2.0	dimensionless	The Hill coefficient of insulin inhibiting lipolysis. It was arbitrarily chosen
ξ	1.5×10^{-4}	$kg \cdot mL \cdot (\mu U)^{-1}$	Suppose the fat mass is 20 kg and because there are 2000 *in silico* adipocytes, the average mass of an adipocyte is at the order of 10^{-2} kg. If the adipocyte's $lg(INS_{on})$ value is 2, then one finds ξ is at the order of $10^{-2}/10^2 = 10^{-4}$

ACKNOWLEDGMENTS

This work was partly supported by the National Natural Science Foundation of China (Nos. 61773196 and 32070681), 2019 Key Projects of Ministry of Science and Technology of China (No. 2019YFA09006000), Guangdong Provincial Key Laboratory of Computational Science and Material Design (No. 2019B030301001), and Shenzhen Research Funds (No. JCYJ20170817104740861), Shenzhen Peacock Plan (No. KQTD2016053117035204), and by Center for Computational Science and Engineering of Southern University of Science and Technology.

COMPLIANCE WITH ETHICS GUIDELINES

The author Guanyu Wang declare that he has no conflict of interests.

This article does not contain any studies with human or animal subjects performed by the author.

REFERENCES

1. Neumann, R. O. (1902) Experimentelle beiträge zur lehre von dem täglichen nahrungsbedarf des menschen unter besonderer berücksichtigung der notwendigen eiweissmenge. Arc. Hyg., 45, 1–87
2. DuBois, E. F. (1924) Basal metabolism in health and disease. AGRIS
3. Sims, E. A. and Horton, E. S. (1968) Endocrine and metabolic adaptation to obesity and starvation. Am. J. Clin. Nutr., 21, 1455–1470
4. Passmore, R. (1971) The regulation of body-weight in man. Proc. Nutr. Soc., 30, 122–127
5. Salans, L. B., Horton, E. S. and Sims, E. A. (1971) Experimental obesity in man: cellular character of the adipose tissue. J. Clin. Invest., 50, 1005–1011
6. Mitchel, J. S. and Keesey, R. E. (1977) Defense of a lowered weight maintenance level by lateral hypothamically lesioned rats: evidence from a restriction-refeeding regimen. Physiol. Behav., 18, 1121–1125
7. Rothwell, N. J. and Stock, M. J. (1979) Regulation of energy balance in two models of reversible obesity in the rat. J. Comp. Physiol. Psychol., 93, 1024–1034
8. Leibel, R. L. and Hirsch, J. (1984) Diminished energy requirements in reduced-obese patients. Metabolism, 33, 164–170
9. Leibel, R. L., Rosenbaum, M. and Hirsch, J. (1995) Changes in energy expenditure resulting from altered body weight. N. Engl. J. Med., 332, 621–628
10. Leibel, R. L. (2008) Molecular physiology of weight regulation in mice and humans. Int. J. Obes., 32, S98–S108
11. Ravussin, Y., Leibel, R. L. and Ferrante, A. W. Jr. (2014) A missing link in body weight homeostasis: the catabolic signal of the overfed state. Cell Metab., 20, 565–572
12. Rosenbaum, M. and Leibel, R. L. (2016) Models of energy homeostasis in response to maintenance of reduced body weight. Obesity (Silver Spring), 24, 1620–1629
13. Kennedy, G. C. (1953) The role of depot fat in the hypothalamic control of food intake in the rat. Proc. R. Soc. Lond. B Biol. Sci., 140, 578–592
14. Anand, B. K. and Brobeck, J. R. (1951) Hypothalamic control of food intake in rats and cats. Yale J. Biol. Med., 24, 123–140
15. Zhang, Y., Proenca, R., Maffei, M., Barone, M., Leopold, L. and Friedman, J. M. (1994) Positional cloning of the mouse obese gene and its human homologue. Nature, 372, 425–432
16. Leibel, R. L. (1997) And finally, genes for human obesity. Nat. Genet., 16, 218–220
17. Friedman, J. M. and Halaas, J. L. (1998) Leptin and the regulation of body weight in mammals. Nature, 395, 763–770
18. Rosenbaum, M. and Leibel, R. L. (1999) The role of leptin in human physiology. N. Engl. J. Med., 341, 913–915
19. Schwartz, M. W., Woods, S. C., Porte, D. Jr, Seeley, R. J. and Baskin, D. G. (2000) Central nervous system control of food intake. Nature, 404, 661–671
20. Myers, M. G. Jr, Münzberg, H., Leinninger, G. M. and Leshan, R. L. (2009) The geometry of leptin action in the brain: more complicated than a simple ARC. Cell Metab., 9, 117–123
21. Rosenbaum, M. and Leibel, R. L. (2014) 20 years of leptin: role of leptin in energy homeostasis in humans. J. Endocrinol., 223, T83–T96
22. Müller, M. J., Geisler, C., Heymsfield, S. B. and Bosy-Westphal, A. (2018) Recent advances in understanding body weight homeostasis in humans. F1000 Res., 7, 7
23. Cohen, S. L., Halaas, J. L., Friedman, J. M., Chait, B. T., Bennett, L., Chang, D., Hecht, R. and Collins, F. (1996) Human leptin characterization. Nature, 382, 589
24. Halaas, J. L., Boozer, C., Blair-West, J., Fidahusein, N., Denton, D. A. and Friedman, J. M. (1997) Physiological response to long-term peripheral and central leptin infusion in lean and obese mice. Proc. Natl. Acad. Sci. USA, 94, 8878–8883
25. Harris, R. B., Hausman, D. B. and Bartness, T. J. (2002) Compensation for partial lipectomy in mice with genetic alterations of leptin and its receptor subtypes. Am. J. Physiol. Regul. Integr. Comp. Physiol., 283, R1094–R1103
26. Zeng, W., Lu, Y.-H., Lee, J. and Friedman, J. M. (2015) Reanalysis of parabiosis of obesity mutants in the age of leptin. Proc. Natl.

Acad. Sci. USA, 112, E3874–E3882
27. Ravussin, Y., Edwin, E., Gallop, M., Xu, L., Bartolomé, A., Kraakman, M. J., LeDuc, C. A. and Ferrante, A. W. Jr. (2018) Evidence for a non-leptin system that defends against weight gain in overfeeding. Cell Metab., 28, 289–299.e5
28. Wang, G. (2020) Body mass dynamics is determined by the metabolic ohms law and adipocyteautonomous fat mass homeostasis. IScience,23, 101176
29. Speakman, J. R. (2018) Why lipostatic set point systems are unlikely to evolve. Mol. Metab., 7, 147–154
30. Perello, M., Scott, M. M., Sakata, I., Lee, C. E., Chuang, J.-C., Osborne-Lawrence, S., Rovinsky, S. A., Elmquist, J. K. and Zigman, J. M. (2012) Functional implications of limited leptin receptor and ghrelin receptor coexpression in the brain. J. Comp. Neurol., 520, 281–294
31. Davis, D. A., Pellowski, D. M., Davis, D. A. and Donahoo, W. T. (2006) Acute and 1-month effect of small-volume suction lipectomy on insulin sensitivity and cardiovascular risk. Int. J. Obes., 30, 1217–1222
32. Kral, J. G. (1976) Surgical reduction of adipose tissue in the male Sprague-Dawley rat. Am. J. Physiol., 231, 1090–1096
33. Hernandez, T. L., Kittelson, J. M., Law, C. K., Ketch, L. L., Stob, N. R., Lindstrom, R. C., Scherzinger, A., Stamm, E. R. and Eckel, R. H. (2011) Fat redistribution following suction lipectomy: defense of body fat and patterns of restoration. Obesity (Silver Spring), 19, 1388–1395
34. Michel, C. and Cabanac, M. (1999) Lipectomy, body weight, and body weight set point in rats. Physiol. Behav., 66, 473–479
35. Giese, S. Y., Bulan, E. J., Commons, G. W., Spear, S. L. and Yanovski, J. A. (2001) Improvements in cardiovascular risk profile with large-volume liposuction: a pilot study. Plast. Reconstr. Surg., 108, 510–519., discussion 520–521.
36. Giese, S. Y., Neborsky, R., Bulan, E. J., Spear, S. L. and Yanovski, J. A. (2001) Improvements in cardiovascular risk profile after large-volume lipoplasty: a 1-year follow-up study. Aesthet. Surg. J., 21, 527–531
37. Crahay, F. and Nizet, J. (2016) Metabolic and Cardiovascular Consequences of Suction-assisted Lipectomy: Systematic Review. In Annales de chirurgie plastique et esthetique, vol. 61270–286
38. Andrew, M. S., Huffman, D. M., Rodriguez-Ayala, E., Williams, N. N., Peterson, R. M. and Bastarrachea, R. A. (2018) Mesenteric visceral lipectomy using tissue liquefaction technology reverses insulin resistance and causes weight loss in baboons. Surg. Obes. Relat. Dis., 14, 833–841
39. Faust, I. M., Johnson, P. R. and Hirsch, J. (1976) Noncompensation of adipose mass in partially lipectomized mice and rats. Americ. J. Phys.-Legac. Cont., 231, 538–544
40. Swanson, E. (2012) Photographic measurements in 301 cases of liposuction and abdominoplasty reveal fat reduction without redistribution Plast. Reconstr. Surg. T., 130, 311e–322e
41. Faust, I. M., Johnson, P. R. and Hirsch, J. (1977) Adipose tissue regeneration following lipectomy. Science, 197, 391–393
42. Hausman, D. B., Lu, J., Ryan, D. H., Flatt, W. P. and Harris, R. B. (2004) Compensatory growth of adipose tissue after partial lipectomy: involvement of serum factors. Exp. Biol. Med. (Maywood), 229, 512–520
43. Mauer, M. M., Harris, R. B. and Bartness, T. J. (2001) The regulation of total body fat: lessons learned from lipectomy studies. Neurosci. Biobehav. Rev., 25, 15–28
44. Spalding, K. L., Arner, E., Westermark, P. O., Bernard, S., Buchholz, B. A., Bergmann, O., Blomqvist, L., Hoffstedt, J., Näslund, E., Britton, T., *et al.* (2008) Dynamics of fat cell turnover in humans. Nature, 453, 783–787
45. Matsuda, N., Hironaka, K.-i., Fujii, M., Wada, T., Kunida, K., Inoue, H., Eto, M., Hoshino, D., Furuichi, Y., Manabe, Y., *et al.* (2020) Monitoring and mathematical modeling of mitochondrial atp in myotubes at single-cell level reveals two distinct population with different kinetics. Quant. Biol., 8, 228–237
46. Chen, L., Liu, R., Liu, Z.-P., Li, M. and Aihara, K. (2012) Detecting early-warning signals for sudden deterioration of complex diseases by dynamical network biomarkers. Sci. Rep., 2, 342
47. Wang, P. and Chen, L. (2020) Critical transitions and tipping points in EMT. Quant. Biol., 8, 195–202
48. Wang, G. (2010) Singularity analysis of the AKT signaling pathway reveals connections between cancer and metabolic diseases Phys. Biol., 7, 046015
49. Wang, G. (2012) Optimal homeostasis necessitates bistable control. J. R. Soc. Interface, 9, 2723–2734
50. Li, T. and Wang, G. (2014) Computer-aided targeting of the PI3K/Akt/mTOR pathway: Toxicity reduction and therapeutic opportunities. Int. J. Mol. Sci. 15, 18856–18891
51. Bonadonna, R. C., Leif, G., Kraemer, N., Ferrannini, E., Prato, S. D. and DeFronzo, R. A. (1990) Obesity and insulin resistance in humans: a dose-response study. Metabolism, 39, 452–459
52. Havel, R. J., Naimark, A. and Borchgrevink, C. F. (1963) Turnover rate and oxidation of free fatty acids of blood plasma in man during exercise: studies during continuous infusion of palmitate-1-C14. J. Clin. Invest., 42, 1054–1063
53. Polonsky, K. S., Given, B. D. and Van Cauter, E. (1988) Twenty-four-hour profiles and pulsatile patterns of insulin secretion in normal and obese subjects. J. Clin. Invest., 81, 442–448
54. Wang, G. (2014) Raison dêtre of insulin resistance: the adjustable threshold hypothesis. J. R. Soc. Interface.11, https://doi.org/10.1098/rsif.2014.0892
55. Bonadonna, R. C., Saccomani, M. P., Cobelli, C. and DeFronzo, R. A. (1993) Effect of insulin on system A amino acid transport in human skeletal muscle. J. Clin. Invest., 91, 514–521
56. Lee, L. (1998) Volume of blood in a human. The Physics Factbook
57. Hall, K. D. (2006) Computational model of *in vivo* human energy metabolism during semistarvation and refeeding. Am. J. Physiol. Endocrinol. Metab., 291, E23–E37
58. Stumvoll, M., Jacob, S., Wahl, H. G., Hauer, B., Löblein, K., Grauer, P., Becker, R., Nielsen, M., Renn, W. and Häring, H. (2000) Suppression of systemic, intramuscular, and subcutaneous adipose tissue lipolysis by insulin in humans. J. Clin. Endocrinol. Metab., 85, 3740–3745